Phase Behavior and Photooptical Properties of Liquid Crystalline Functionalized Copolymers with Low-Molecular-Mass Dopants Stabilized by Hydrogen Bonds

A. V. Medvedev, E. B. Barmatov,* A. S. Medvedev, and V. P. Shibaev

Department of Chemistry, Moscow State University, Moscow 119992, Russia

S. A. Ivanov

Physical Department, Moscow State University, Moscow 119992, Russia

M. Kozlovsky

Institut fur Physikalische Chemie, Technische Universitat Darmstadt, Petersenstrase 20, D-64287 Darmstadt, Germany

J. Stumpe

Fraunhofer Institute of Applied Polymer Research, Geiselbergstrasse 69, Golm 14476, Germany

Received September 3, 2004; Revised Manuscript Received December 18, 2004

ABSTRACT: The approach of deriving new photooptically active polymeric substances by hydrogen bonding between functionalized liquid crystalline (LC) copolymers and low-molecular-mass dopants, containing photochromic azobenzene fragments, is described. The formation of intermolecular hydrogen bonds between carboxylic groups of functionalized LC copolymers and the pyridine fragment of the dopant leads to stable, nonseparating mixtures in a broad interval of contents (up to 30 mol % dopant molecules). The phase behavior and structure of photochromic mixtures are investigated. Induction of a nematic mesophase is observed in the case of a smectic polymer matrix doped with low-molar-mass photochromic dyes.

Introduction

Synthesis of functionalized liquid crystalline (LC) polymers constitutes one of the challenging issues of modern physical chemistry of polymers.[1] As is known, copolymerization of mesogenic and nonmesogenic monomers provides the classical means for the preparation of the above compounds when one macromolecule contains various monomer units of different chemical natures and functionalities. At the same time, such systems may also be obtained via specific noncovalent interactions of LC copolymers containing carboxyl groups with low-molecular-mass compounds (dopants) with valuable characteristics.[2−4] This approach allows the development of a new generation of advanced composite materials and their application in optoelectronics, holography, data recording, and imaging systems. The above blends may advantageously combine the properties of polymers (film-forming and fiber-forming properties as well as their ability to produce coatings) and low-molecular-mass dopants (photochromism, high optical activity, and high response to the action of magnetic fields).

Functionalized LC polymers may be used as suitable matrixes for further controlled design of their characteristics via modification by low-molecular-mass dopants, including dopants containing either chiral[5] or photochromic groups.[6]

The objective of this work is focused on working out the approach for the preparation of functionalized LC polymer blends based on comb-shaped LC polymers and hydrogen-bonded photochromic dopants, on studying their phase behavior and structure, and on investigating their photooptical properties under the action of polarized laser irradiation. We studied functionalized acrylic LC copolymers containing different concentrations of mesogenic and carboxyl groups. The content of acidic groups in the copolymer (mol %) was the following: $y = 28-78$ mol % and $x = 100 - y$.

Polymers

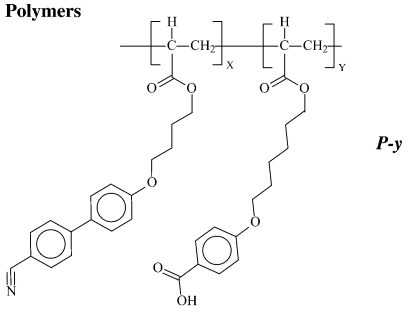

P-y

Photochromic dopants

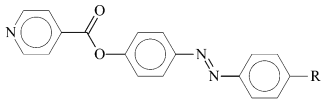

PyAzoR

R=H (***PyAzo***),

R=CN (***PyAzoCN***)

R=OCH3 (***PyAzoOMe***)

R=C4H9 (***PyAzoBu***)

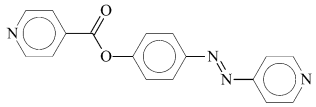

PyAzoPy

* To whom correspondence should be addressed. E-mail: barmatov@genebee.msu.su. Phone: (095) 939-3132. Fax: (095) 939-0174.

10.1021/ma048192w CCC: $30.25
Published on Web 02/08/2005

Table 1. Molecular Mass Characteristics and Temperatures of Phase Transitions (Transition Heats (J/g) Are Given in Parentheses) of the Functionalized LC Copolymers P-*y*

copolymer	$M_w \times 10^{-3}$	M_w/M_n	phase transitions, °C
P-28	5.9	1.7	glass 32 N 95 (1.2) I
P-39	5.4	1.8	glass 30 SmA 110 (3.4) I
P-51	7.2	1.6	glass 32 SmA 154 (3.4) I
P-61	6.2	1.7	glass 36 SmA 130 (4.2) I
P-78	7.4	1.8	glass 39 SmA 145 (3.8) I

The presence of a pyridine ring in the chemical structure of the dopant molecules is responsible for the development of donor−acceptor hydrogen bonds (pyridine serves as a proton acceptor, and alkyloxybenzoic acid as a proton donor); as a result, high compatibility between the components of the blend is provided by the formation of a new extended mesogenic group which is shown below:

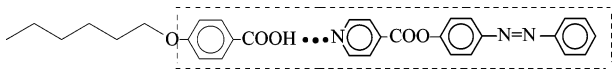

The selected dopants contain an azobenzene fragment which is capable of isomerization and further photoinduced orientation under the action of polarized laser irradiation. Hence, one may expect that the prepared compounds may be used as promising materials for optical data recording and storage. Low-molecular-mass dopants with different substituents at the 4′-position of the azobenzene fragment were synthesized. This approach makes it possible to study the effect of the chemical structure of the dopants on the phase behavior of the above blends. The low-molecular-mass PyAzoPy dopant is able to form two hydrogen bonds and, thus, may serve as a bridge fragment between two carboxyl groups of the copolymer.

Experimental Section

LC copolymers were prepared by the free radical copolymerization of 4-(4-cyanodiphenyl-4′-yloxy)butyl acrylate (M1) with 4-[6-(acryloyloxy)hexyloxy]benzoic acid (M2). The polymerization was carried out in a 10 wt % monomer concentration of absolute THF at 60 °C over 48 h under nitrogen. AIBN was used as an initiator (2 wt %). The yield was 76−85%. The concentration of M2 in the monomer feed was 30−80 mol %. The synthesized copolymers were precipitated from a THF solution by hexane. The copolymer composition was determined by elemental analysis and NMR spectroscopy (Supporting Information). The composition, molecular mass characteristics, and phase transitions of the copolymers are presented in Table 1.

All monomers and dopants were synthesized according to the earlier described procedures.[5b] Some characteristics of the dopants used are outlined below.

M1. Cr 93 (N 50) I. NMR ($CDCl_3$): δ 7.97 (d, 2H, Ph, J = 8.85 Hz); 7.67 (d, 2H, Ph, J = 8.55 Hz); 7.62 (d, 2H, Ph, J = 8.51 Hz); 7.51 (d, 2H, Ph, J = 8.81 Hz); 6.35 (dd, 1H, CH_2=CH−, J = 1.65, 17.65 Hz); 6.12 (dd, 1H, CH_2=CH−, J = 10.3, 17.31 Hz); 5.81 (dd, 1H, CH_2=CH, J = 1.65, 10.3 Hz); 4.21 (t, 2H, OCH_2); 4.02 (t, 2H, −CH_2O); 1.89 (4H, −CH_2CH_2−).

M2. Cr 85 SmA 96 N 103 I. NMR ($CDCl_3$): δ 7.95 (d, 2H, Ph, J = 8.82 Hz); 6.93 (d, 2H, Ph, J = 8.82 Hz); 6.35 (dd, 1H, CH_2=CH−, J = 1.65, 17.65 Hz); 6.12 (dd, 1H, CH_2=CH−, J = 10.3, 17.31 Hz); 5.81 (dd, 1H, CH_2=CH−, J = 1.65, 10.3 Hz); 4.3 (t, 2H, OCH_2−); 4.12 (t, 2H, −CH_2O); 1.3−1.9 (8H, −CH_2−).

PyAzoCN. Cr 160 N 192 I. λ_{max} = 357 nm ($CHCl_3$). NMR ($CDCl_3$): δ 8.9 (d, 2 H); 8.02 (m, 6 H); 7.81 (d, 2 H); 7.42 (d, 2 H).

PyAzoPy. Cr 185−186 I. λ_{max} = 335 nm ($CHCl_3$). NMR ($CDCl_3$): δ 8.9−8.8 (m, 4H); 8.15 (m, 6 H); 7.7 (m, 2 H).

PyAzoOMe. K1 148 K2 163 N 197 I. λ_{max} = 351 nm ($CHCl_3$). NMR ($CDCl_3$): δ 8.84 (d, 2 H); 8.3 (m, 2 H); 8,04 (d, 4 H); 7.86 (d, 2 H); 7.83 (d, 2 H); 7.26 (d, 2 H); 6.88 (d, 2 H); 3.83 (s, 3 H).

PyAzoBu. K 124 N 130 I. λ_{max} = 337 nm ($CHCl_3$). NMR ($CDCl_3$): δ 8.83 (d, 2 H); 8.1 (m, 6 H); 7.63 (d, 2 H); 7.2 (d, 2 H), 2.52 (t, 2 H), 1.4 (m, 4H), 0.92 (s, 3H).

PyAzo. K 146 I. λ_{max} =325 nm ($CHCl_3$). NMR ($CDCl_3$): δ 8.85 (d, 2 H); 8.06 (m, 4 H); 7.95 (d, 2 H); 7.54 (m, 3 H); 7.4 (d, 2 H).

Blends P-*y*−PyAzoR (*z*) (*z* is the mole fraction of photochromic dopant PyAzoR in the blends: z = [dopant]/([copolymer] + [dopant])

were obtained using the following procedure. To the solution of copolymer P-*y* in freshly distilled anhydrous THF was added the calculated amount of dopant dissolved in anhydrous THF. The mixture was mixed on the magnetic stirrer for 1 h at room temperature. After that, the solvent was evaporated on a rotor evaporator and then dryed in a vacuum at 110 °C at 2 h.

Microcalorimetry studies were performed with a "Mettler" differential scanning calorimeter (TA4000) at a scanning rate of 10 °C min^{-1} from −10 to +180 °C in nitrogen. The DSC cell was calibrated with indium. Polarizing optical microscopy observations were made with a Zeiss polarizing microscope equipped with a Mettler FP-82HT hot stage controlled by a Mettler FP90 unit. X-ray diffraction (XRD) patterns were obtained from a 2 mm diameter capillary sample with a modified STOE STADI 2 diffractometer using Ni-filtered Cu Kα radiation (40 kV, 30 mA) and a PSD linear position scanning detector. A 2θ scanning speed of 1 deg min^{-1} with a sampling interval of 0.01° was used.

The UV spectra were recorded by a Unicam UV 500 spectrometer in the region 250−900 nm at a spectral resolution of 2 nm. The IR spectra were recorded by an FTIR spectrometer (Biorad FTS 6000) in the region 400−4000 cm^{-1} at a spectral resolution of 1−4 cm^{-1} and an uncertainty of <5% in absorbance. For the absorbance measurements the samples were confined on KBr windows. ^{1}H NMR spectra were measured in a 4−8 wt % DSMO-d_6 solution by an NMR spectrometer (JEOL GSX-400) at 400 MHz. Tetramethylsilane was used as an internal reference. The kinetics of photoinduced birefringence was studied on a photooptical setup described in detail in ref 7.

The relative molecular weights of the polymers were determined by gel permeation chromatography (GPC) using a GPC-2 Waters instrument equipped with an LC-100 column oven and a Data Modul-370 data station. Measurements were made by using a UV detector, THF as solvent (1 mL/min, 25 °C), a set of PL columns of 100, 500, and 10^3 Å, and a calibration plot constructed with polystyrene standards.

Results and Discussion

IR Spectroscopy of Hydrogen-Bonded Blends. Hydrogen bonding in functionalzed LC copolymers and blends with dopant PyAzoCN was investigated by IR spectroscopy. Figure 1 shows the characteristic IR spectrum of LC copolymer P-51 in the region of 1550−1800 cm^{-1}. Several overlapping bands can be seen in the carbonyl region. The monomer unit of alkyloxybenzoic acid exhibits two characteristic bands at 1684 and 1744 cm^{-1} assigned to stretching vibrations of the carbonyl, $\nu_{C=O}$, in the carboxylic group. The 1744 cm^{-1} bend is assigned to the "free" (monomer) form and that at 1684 cm^{-1} to the dimer form of the acid;[5,6] the band at 1728 cm^{-1} is assigned to a stretching vibration, $\nu_{C=O}$, of the ester groups. The incorporation of PyAzoCN groups into polymer matrix P-51 leads to disappearance of the band at 1744 cm^{-1} and to the growth of the 1684 cm^{-1} band intensity, proving hydrogen bond formation between the initial compounds. The formation of hy-

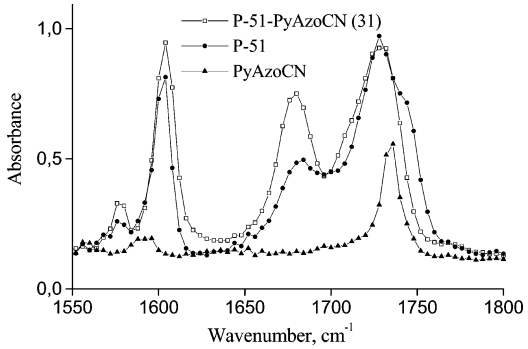

Figure 1. IR spectra of the functionalized LC copolymer P-51 and azobenzene-containing dopant PyAzoCN and their blend P-51−PyAzoCN (31).

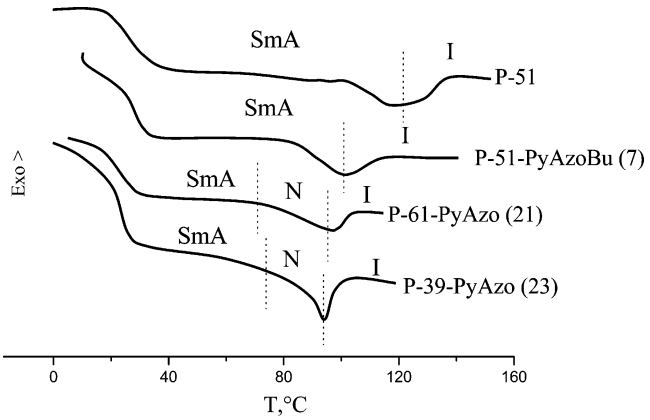

Figure 2. DSC curves of the copolymer and blends.

drogen bonds is confirmed for all blends under investigation.

Phase State of the Blends. The phase behaviors of the initial LC copolymers and their blends were studied by the method of polarization microscopy, DSC, and X-ray analysis. The nematic phase was identified as the appearance of a marble texture. The formation of the SmA phase is proved by the emergence of a fanlike texture (Supporting Information) as well as by the presence of small-angle X-ray reflections at the corresponding X-ray diffractograms of the blends.

Figure 2 presents the typical DSC curves for copolymers and their blends containing dopants. The SmA−isotropic melt transition in the copolymers and related blends is accompanied by the appearance of a wide temperature interval where a two-phase structure exists (10−15 °C); in the DSC curve, this transition appears as a wide endothermic peak with a fusion heat of 2.4−4.8 J/g. The nematic−isotropic melt transition is characterized by a much lower fusion heat (ΔH = 0.9−1.4 J/g). Figure 3a presents the X-ray diffractograms of the blend based on polymer matrix P-51 and the PyAzoBu dopant. With increasing concentration of dopant, the character of the SmA packing of side mesogenic and photochromic groups remains virtually unchanged. As the concentration of dopant PyAzoR is increased, interplanar distances are somewhat increased (Figure 3b).

Effect of the Concentration and Molecular Structure of a Low-Molecular-Mass Dopant on the Phase Behavior of the Blends. Figure 4 presents the phase diagrams for the P-*y*−PyAzo blends. First, one should mention that, when the dopant concentration does not exceed 30 mol %, no phase separation takes

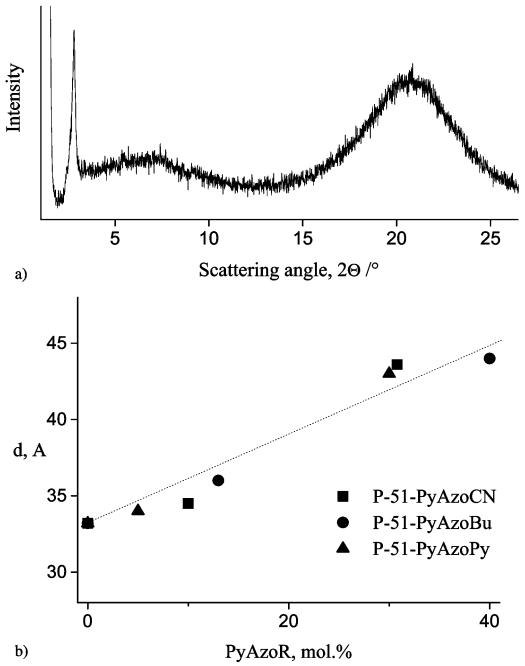

Figure 3. Diffractogram of the P-51−PyAzoBu (13) blend at room temperature (a) and concentration dependence of the interplanar spacing *d* for the SmA phase of P-51−PyAzoR blends (b).

place. Phase separation does not occur even upon their prolonged annealing (for several days) at different temperatures. The corresponding DSC curves reveal only transitions related to the melting of the LC phase. Therefore, one may conclude that the above blends formed via hydrogen bonding do behave as individual compounds in a wide range of their compositions. In the case of the P-51−PyAzoR blends containing about 40 mol % dopant, a crystalline phase is formed. Simple calculation shows that, for a copolymer containing 50 mol % acidic groups, one acidic group of the copolymer corresponds to one dopant molecule at a molar content of the dopant of 33 mol %. Therefore, the formation of a crystalline phase in the P-51−PyAzoR blends is related to the crystallization of excessive dopant which is free of any hydrogen bonds.

In some cases, with increasing content of crystalline dopant PyAzo in the copolymer, the clearing temperature T_{cl} is somewhat increased. This behavior may be explained as follows. The development of hydrogen bonds between an acidic group and a pyridine group via the donor−acceptor mechanism entails the formation of a new extended fragment with mesogenic properties. As was shown by Kato and Frechet,[2] the formation of a new extended mesogenic group may be accompanied by an increase in T_{cl} of the blends and by the emergence of more ordered phases as compared with the initial components.

To gain a deeper insight into the details of the phase behavior of the systems stabilized by hydrogen bonds, the mixtures of *n*-hexyloxybenzoic acid (A6) with dopant PyAzoCN were studied; such mixtures model the formation of an extended mesogenic group and serve as a low-molecular-mass analogue of P-*y*−PyAzoR polymer blends. Figure 5 presents the DSC curves for the mixtures of A6 and dopant PyAzoCN. For all components and their mixtures, the corresponding DSC curves clearly show a well-pronounced melting peak of the crystalline phase. The N−isotropic melt transition for *n*-hexyloxybenzoic

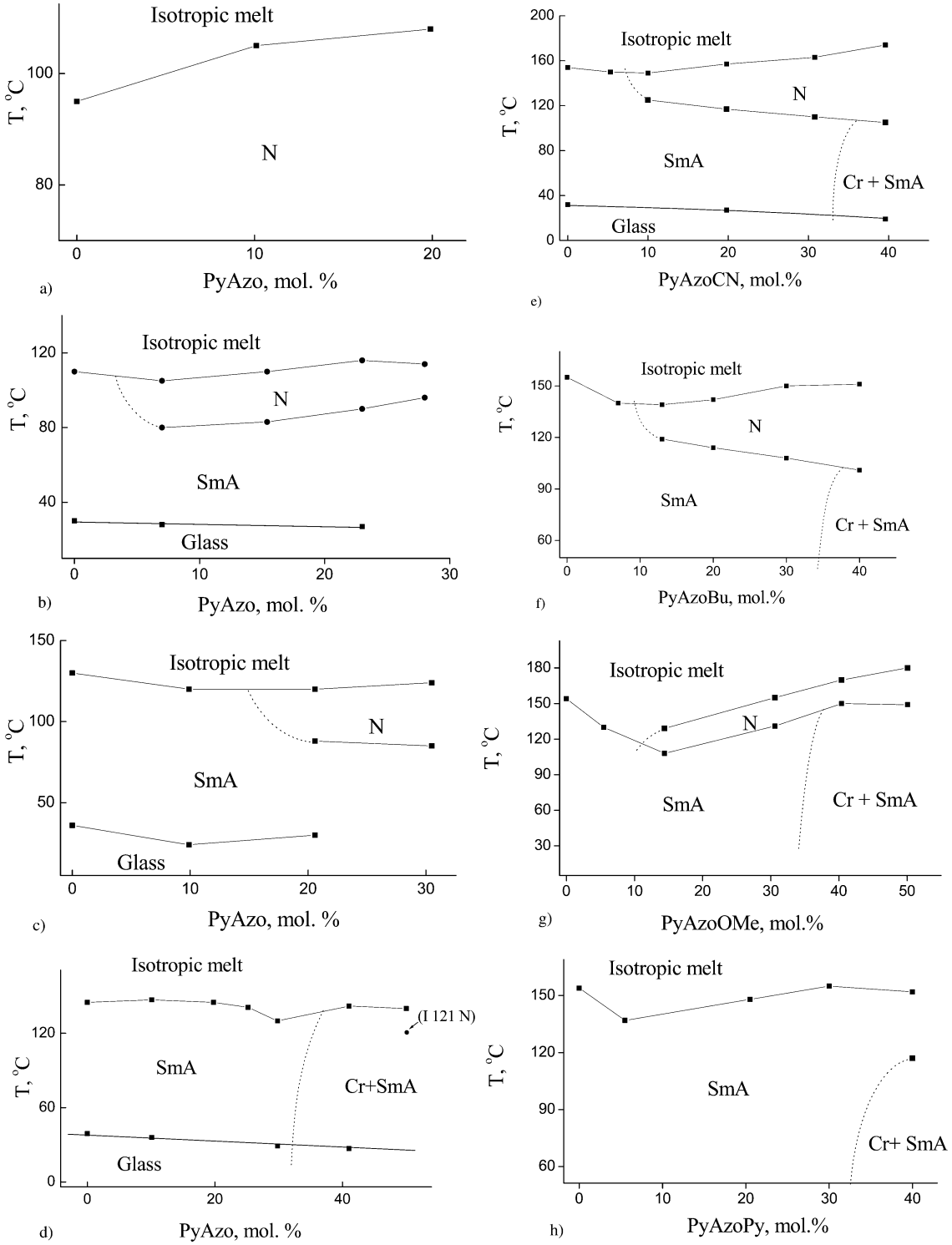

Figure 4. Phase behaviors of blends P-28−PyAzo (a), P-39−PyAzo (b), P-61−PyAzo (c), P-78−PyAzo (d), P-51−PyAzoCN (e), P-51−PyAzoBu (f), P-51−PyAzoOMe (g), and P-51−PyAzoPy (h).

acid and PyAzoCN and their mixtures appears in the corresponding DSC scans as a peak with a fusion heat of 1.7−11 J/g. In the case of the SmA−N transition, the fusion heat is equal to 0.6−1.5 J/g.

Analysis of the behavior of low-molecular-mass mixtures of *n*-hexyloxybenzoic acid and dopant PyAzoCN also suggests that clearing temperatures increase with increasing content of photochromic dopant PyAzoCN (Figure 6). Furthermore, when the content of PyAzoCN is equal to 20−40 mol %, one may observe the development of a smectic phase even though both starting components are characterized by a nematic type of ordering. This evidence testifies that a new extended mesogenic group is formed, and its appropriate anisodiametry is higher than those of the initial components.

Therefore, the phase behaviors of the hydrogen-bonded polymer blends P-28−PyAzo and low-molecular-mass model mixtures A6−PyAzoCN appear to be appreciably different. In contrast to low-molecular-mass mixtures P6−PyAzoCN, the introduction of PyAzo dopant molecules to nematic copolymer P-28 does not lead to any generation of its smectic phase (Figure 4a).

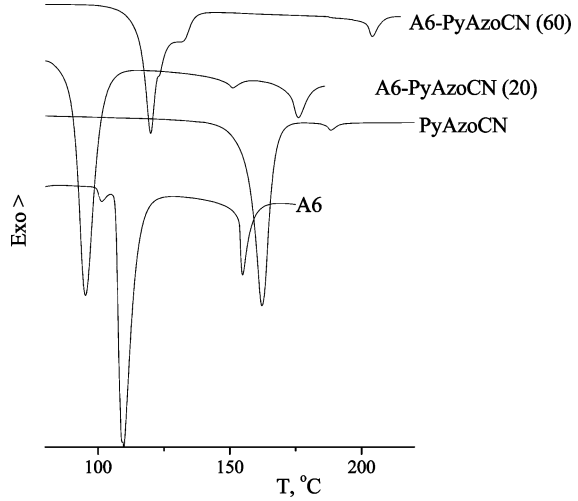

Figure 5. DSC curves of the modeling low-molecular-mass mixtures A6−PyAzoCN.

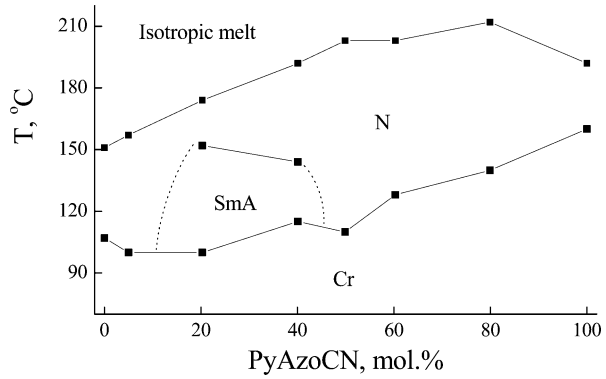

Figure 6. Phase behavior of blends of PyAzoCN and *n*-hexyloxybenzoic acid (A6).

In this work, we describe the unusual effect of hydrogen bonding on the phase state of the blends. When the blends of nematic LC copolymer P-28 with dopant PyAzo are able to form only their nematic phase (Figure 4a), introduction of PyAzo molecules to the smectic P-39 matrix changes the whole "phase set" of the blend. When the concentration of PyAzo is equal to ~10 mol %, in addition, one may observe both SmA and nematic phases (Figure 4b); in this case, the temperature interval of the nematic phase and glass transition temperature of P-39−PyAzo blends slightly depend on the concentration of the dopant.

To explain the above behavior, we propose a model that describes the emergence of a nematic phase in blends based on smectic copolymers. This model involves two key issues.

First, as follows from the above experimental evidence, the development of hydrogen bonds between acid and pyridine leads to a breakdown of the system of intermolecular hydrogen bonds in the initial copolymer P-*y*, which is responsible for SmA packing of the side groups (structure A, Figure 7). In this case, the formation of an extended mesogenic group via hydrogen bonding should be accompanied by an increase in the thickness of the smectic layer (structure B, Figure 7); as a result, the cooperative lateral interactions of the mesogenic groups become weaker, and lamellar packing breaks down.

Second, hydrogen-bonded mesogenic groups are characterized by much lower values of the order parameter

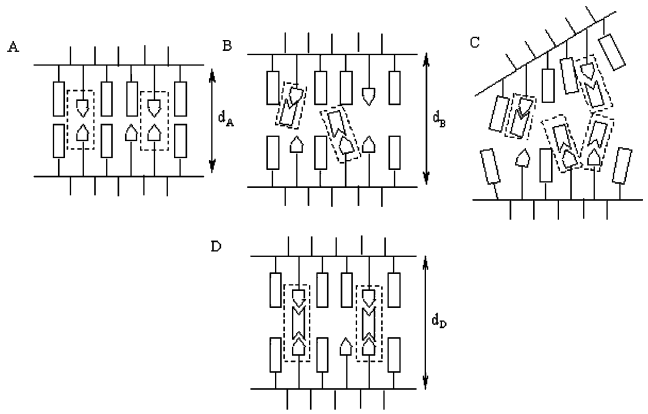

Figure 7. Model of packing of mesogenic (rectangle), functional alkyloxybenzoic (pentagon), and photochromic (rectangle with a triangle taken out of one end) groups in copolymer P-*y* and blends ($d_A < d_B$; d is the interplanar spacing of the SmA phase).

S as compared with those of mesogenic fragments of the copolymer.[8] This conclusion directly follows from the ^{2}H NMR spectroscopic study of the orientational behavior of hydrogen-bonded blends of LC copolymers containing carboxyl groups with low-molecular-mass pyridine-containing dopants under the action of the magnetic field. All factors assist the formation of a less ordered nematic phase due to the introduction of a crystalline dopant to the smectic copolymer (structure C, Figure 7).

This model is proved by a well-pronounced dependence of smectic layer thickness on dopant content. As is well seen, introduction of various dopants to polymer matrix P-51 is accompanied by an increase in the interplanar distance *d* (Figure 3b). For example, for the P-51−PyAzoCN blend containing 30 mol % dopant PyAzoCN, *d* increases by 10 Å.

Therefore, one may conclude that dopant molecules exert a destabilizing effect on the phase state of LC copolymers. At the same time, one may reduce this destabilizing effect of the dye molecules by using LC copolymers with a high content of acidic groups relative to the content of dopant molecules. Indeed, for copolymer P-61 containing 60 mol % acidic groups, the critical concentration of dopant PyAzo required for the development of a nematic phase increases from ~8 mol % (for copolymer P-39) to ~22 mol % (Figure 4c). Furthermore, for a copolymer containing 80 mol % acidic groups, one may observe the formation of a monotropic nematic phase at a dopant content of 49 mol % (Figure 4d).

Far more important results supporting the proposed model were obtained for the blends of P-51 and dopant PyAzoPy containing two pyridine rings; this dopant is able to form two hydrogen bonds with acidic groups of copolymers involved in the development of a smectic layer and acts as a "cross-linking" agent (structure D, Figure 7). Even though introduction of dopant PyAzoPy to copolymer P-51 is accompanied by an increase in interplanar distances (Figure 3b), the initial smectic structure of the copolymer is preserved when the content of PyAzoPy varies from 5 to 40 mol % (Figure 4g). This fact confirms a key role of intermolecular hydrogen bonds in the formation of a smectic layer in copolymers P-*y* and P-*y*-PyAzoPy blend (structures A and D, Figure 7).

Let us consider how the chemical nature of the end group of dopant PyAzoR affects the phase state of the

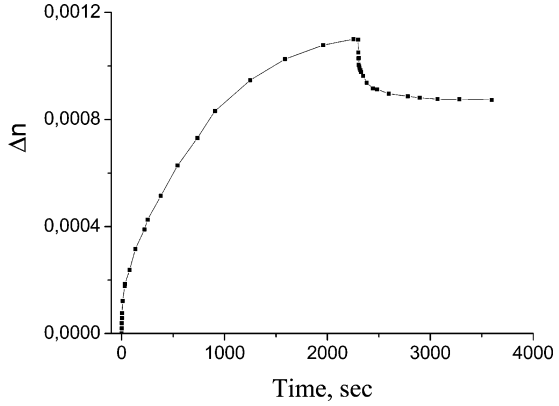

Figure 8. Increasing birefringence under laser irradiation in a P-39−PyAzo (15) homeotropic film at room temperature. The dashed lines indicate the moment when the laser irradiation was switched off (P = 0.15 W/cm^2).

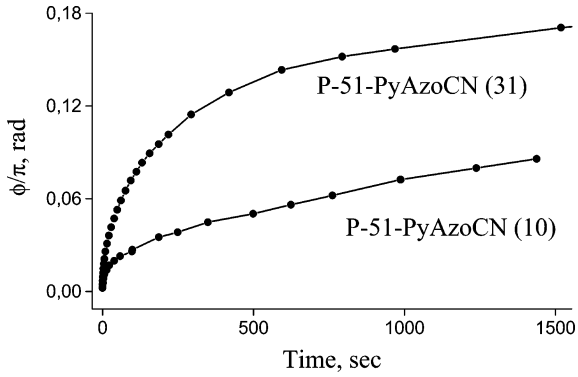

Figure 9. Kinetic curves of the growth of the phase shift φ/π vs the irradiation time of blends at room temperature for blends P-51−AzoPyCN (10) and P-51−AzoPyCN (31) (488 nm, P = 0.12 W/cm^2).

blends and the ability of the dopant to induce the formation of a nematic phase. Figure 4e−g shows the phase diagrams of blends based on the same copolymer P-51 but containing different dopants. The analysis of the above phase diagrams suggests that dopants containing various polar substituents (−H, −CN, −Bu, −OMe) at the 4′-position of azobenzene do not bring any marked changes in the phase state of the blends under study. In all cases, a nematic phase is formed. Therefore, the above effect is virtually independent of the chemical nature of the end groups of dopant PyAzoR.

Photooptical Properties. Let us consider the basic features of the photooptical behavior of photochromic blends stabilized by specific noncovalent interactions. Figure 8 shows the kinetic curves describing an increase in photoinduced birefringence for the samples based on hydrogen-bonded blends. Laser irradiation leads to the appearance and increase of birefringence. Photoinduced birefringence for a homeotropically oriented film is equal to about 10^{-3}, and this value agrees with the literature data on the photoorientation of photochromic LC copolymers containing photochromic fragments with virtually identical chemical structures.[7] When irradiation is switched off, birefringence decreases (∼10−20%) within ∼300−600 s; then, this level is preserved for a long period of time.

Figure 9 shows the photoinduced birefringence plotted against the concentration of the photochromic dopant. In this case, the kinetic curves describing birefringence growth are presented as time dependences of the phase shift φ/π between reading beam components which are

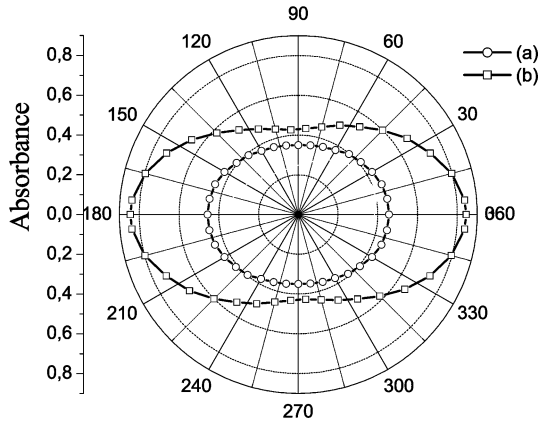

Figure 10. Polar diagram at 350 nm for (a) P-51−AzoPyCN (10) and (b) P-51−AzoPyCN (31) blends after polarized laser irradiation (P = 100 mW/cm^2, 1 h).

parallel and perpendicular to the electric vector of the recording beam. As is seen, with increasing content of the photochromic dopant in the blend, photoinduced birefringence increases.

The UV polarization spectroscopic data also prove the emergence of dichroism in the films of blends as well as illustrate how orientation of side mesogenic groups in the direction perpendicular to the direction of the electric vector of light irradiation depends on the dopant content (Figure 10). As is well seen, the photoinduced dichroism increases with increasing content of the photochromic component in the blend. For example, for the sample containing 31 mol % dopant PyAzoCN, photoinduced dichroism is equal to 0.33, whereas, for the sample containing 10 mol % dopant, dichroism is equal only to 0.13.

Therefore, comparison of the photooptical behavior of functionalized photochromic blends with the literature data on the photoptical behavior of photochromic LC copolymers[7] reveals their striking similarity. This similarity appears as identical kinetic curves describing both an increase and a decrease in photoinduced birefringence as well as similar dependences of birefringence on the orientation of the test samples and content of the photochromic groups.

Acknowledgment. This work was supported by RFBR (Grant 04-03-32464 and 04-03-32461).

Supporting Information Available: Polarized optical textures for LC copolymers and blends and ^{1}H NMR spectra of LC copolymers P-*y*. This material is available free of charge via the Internet at http://pubs.acs.org.

References and Notes

(1) (a) McArdle, C., Ed. *Side chain liquid crystal polymers*; Blackie: London, 1989. (b) *Handbook of liquid crystals*; Demus, D., Goodby, J., Grey, G. W., Spiess, H. W., Vill, V., Eds.; Wiley-VCH: New York, 1998; Vols. I−IV.

(2) (a) Kato, T.; Frechet, J. M. J. *Macromolecules* **1989**, *22*, 3818. (b) Kato, T.; Frechet, M. J. *Macromol. Symp.* **1995**, *98*, 311. (c) Kato, T. *Hydrogen-Bonded Systems in Handbook of Liquid Crystals, IIB*; Wiley-VCH: Weinheim, Germany, 1997; p 969. (d) Paleos, C. M.; Tsiourvas, D. *Angew. Chem., Int. Ed. Engl.* **1995**, *34*, 1696. (e) Brandys, F. A.; Bazuin, C. G. *Chem. Mater.* **1996**, *8*, 83. (f) Kihara, H.; Kishi, R.; Miura, T.; Kato, T.; Ichijo, H. *Polymer* **2001**, *42*, 1177.

(3) (a) Shatalova, A. M.; Shandryuk, G. A.; Bondarenko, G. B.; Kuptsov, S. A.; Talroze, R. V.; Plate N. A. *Polym. Sci. A* **2003**, *45*, 135. (b) Shandryuk, G. A.; Kuptsov, S. A.; Shatalova, A.

M.; Plate, N. A.; Talroze, R. V. *Macromolecules* **2003**, *36*, 3417.

(4) (a) Kaneko, T.; Yamaoka, K.; Gong, J. P.; Osada, Y. *Macromolecules* **2000**, *33*, 412. (b) Yamaoka, K.; Kaneko, T.; Gong, J. P.; Osada, Y. *Macromolecules* **2001**, *34*, 1470. (c) Kaneko, T.; Nagasawa, H.; Gong, J. P.; Osada, Y. *Macromolecules* **2004**, *37*, 187. (d) Mihara, T.; Kokubun, T.; Koide, N. *Mol. Cryst. Liq. Cryst*. **1999**, *330*, 235.

(5) (a) Barmatov, E. B.; Bobrovsky, A. Yu.; Barmatova, M. V.; Shibaev, V. P. *Polym. Sci.* **1998**, *40*, 1769. (b) Barmatov, E. B.; Bobrovsky, A. Yu.; Barmatova, M. V.; Shibaev, V. P. *Liq. Cryst*. **1999**, *26*, 581. (c) Barmatov, E. B.; Bobrovsky, A. Yu.; Pebalk, D. A.; Barmatova, M. V.; Shibaev, V. P. *J. Polym. Sci., Part A: Polym. Chem.* **1999**, *37*, 3215. (d) Barmatov, E. B.; Obrascov, A. A.; Pebalk, D. A.; Barmatova, M. V. *Colloid Polym. Sci.* **2004**, *282*, 530. (e) Barmatov, E. B.; Barmatova, M. V. *Liq. Cryst*. **2003**, *30*, 1075.

(6) (a) Stewart, D.; Imrie, C. T. *Macromolecules* **1997**, *30*, 877. (b) Wu, X.; Zhang, G.; Zhang, H. *Macromol. Chem. Phys*. **1998**, *199*, 2101. (c) Barmatov, E. B.; Medvedev, A. V.; Ivanov, S. A.; Barmatova, M. V.; Shibaev V. P. *Polym. Sci.* **2001**, *43A*, 285.

(7) Shibaev, V. P.; Kostromin, S. G.; Ivanov, S. A. *Polym. Sci.* **1997**, *39A*, 36.

(8) (a) Barmatov, E.; Grande, S.; Filippov, A.; Barmatova, M.; Kremer, F.; Shibaev, V. *Macromol. Chem. Phys.* **2000**, *201*, 2603. (b) Barmatov, E. B.; Filippov, A. P.; Shibaev, V. P. *Liq. Cryst.* **2001**, *28*, 511.

MA048192W